Supporting Information

Recombinant hyaluronic acid-incorporated self-healing injectable hydrogel for cartilage tissue engineering: A case study on effects of molecular weight

Manoj Kumar Sundaram[1], Chelladurai Karthikeyan Balavigneswaran[2]*, Iniyan Saravanakumar[1], Guhan Jayaraman[1], Vignesh Muthuvijayan[1]*

[1]Department of Biotechnology, Bhupat and Jyoti Mehta School of Biosciences Building, Indian Institute of Technology Madras, Chennai 600036, India

[2] Centre for Nanobiotechnology, Vellore Institute of Technology (VIT) Vellore-632014, Tamil Nadu, India

*Corresponding author E-mail: balaa02@gmail.com, vigneshm@iitm.ac.in

Production, purification, and characterization of HA:

Metabolically engineered strains of *Lactococcus lactis* were cultured in 2 L of modified M17 medium. In the bioreactor, HA synthesis was induced with 2 ng/mL of nisin when the optical density at 600 nm (OD_{600}) reached 0.6. At the end of fermentation, the culture broth was treated with SDS and centrifuged. The strains and conditions of HA production for the various molecular weights are mentioned in Table S1.

Table S1. Strains and fermentation conditions used for producing HA of various molecular weights

S.No	Strain Name	Glucose Concentration	Bioreactor strategy	HA MW (MDa)	References
1	*L. lactis* NZ9000 GJP2	10 g/L	Glucostat	0.5	[1]
2	*L. lactis* NZ9000 GJP2	30 g/L	Glucostat	1.0	[1]
3	*L. lactis* MKG6	30 g/L	Batch	2.0	[2]

Firstly, the diafiltration method effectively concentrated HA while removing impurities from the fermentation broth for tissue engineering applications. Secondly, the GPC analysis provided precise molecular weight distributions for HA. The retention times obtained from gel permeation chromatography (GPC) analysis provide critical insights into the molecular weight distribution of hyaluronic acid (HA) samples derived from *Lactococcus lactis*, which were subsequently utilized for hydrogel preparation. The HA samples with molecular weights of 0.5 MDa, 1 MDa, and 2 MDa exhibited retention times of 12 minutes, 14 minutes, and 14.6 minutes, respectively (Figure S1).

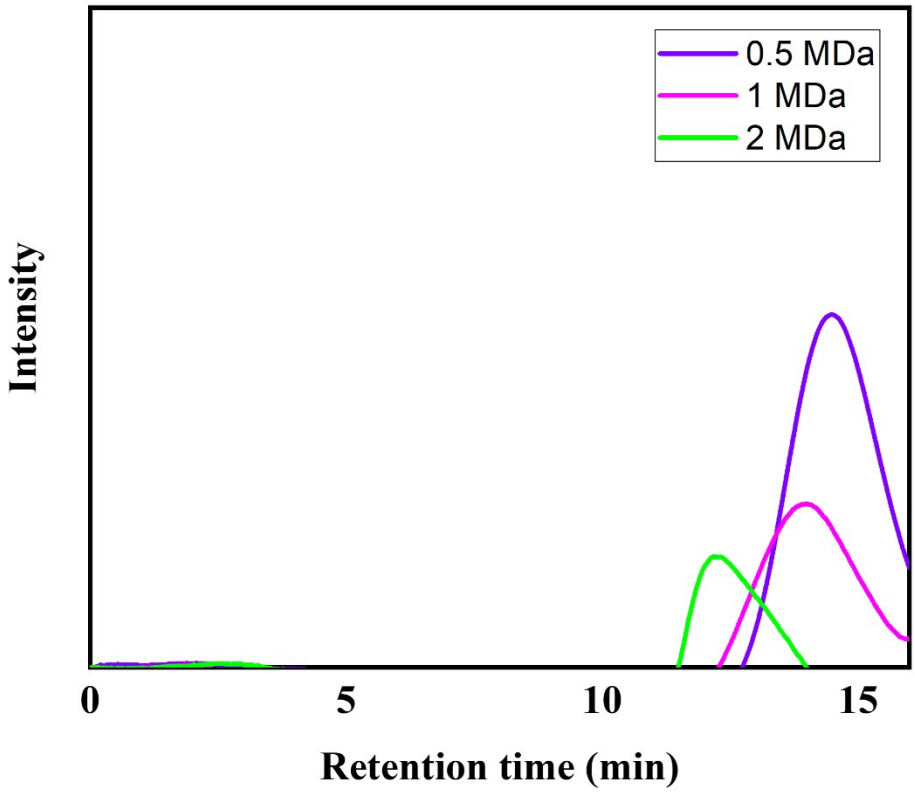

Figure S1. GPC analysis of hyaluronic acid (HA) samples derived from *Lactococcus lactis* showing molecular weight distributions. HA samples with molecular weights of 0.5 MDa, 1 MDa, and 2 MDa exhibited retention times of 12, 14, and 14.6 minutes, respectively.

Synthesis and characterization of oxidized alginate:

The synthesis scheme is illustrated in Figure S2. Briefly, sodium alginate (5 g, 23 mmol) was dissolved in 100 mL of water, and sodium periodate (2.6 g, 12.5 mmol) was added to achieve 50% oxidation. The mixture was stirred in darkness for 6 h to yield oxidized alginate. The reaction was then terminated by the addition of ethylene glycol. The product was precipitated in ethanol and redissolved in distilled water to eliminate impurities such as sodium periodate and unreacted sodium alginate.

UV-visible spectroscopy was performed using a Jasco V650 spectrophotometer (JASCO Corporation, Japan) to analyze the optical properties of the samples. The absorbance spectra were recorded at room temperature in the wavelength range of 190-300 nm. The spectral data were analyzed to identify characteristic absorption peaks and determine the optical properties of the samples. FTIR analysis of the synthesized hydrogels was performed using Fourier Transform infrared (FTIR) spectroscopy (PerkinElmer, USA) in the transmittance mode. The transmittance readings were measured by accumulating 32 scans at a resolution of 4 cm^{-1} in the spectral region of 4000−400 cm^{-1}. The ^{1}H NMR spectra were recorded using a Bruker Avance 500 MHz spectrometer at room temperature, with D2O as the solvent. Chemical shifts (δ) are reported in parts per million (ppm), referenced to either the internal standard tetramethylsilane (TMS) or the residual solvent peak.

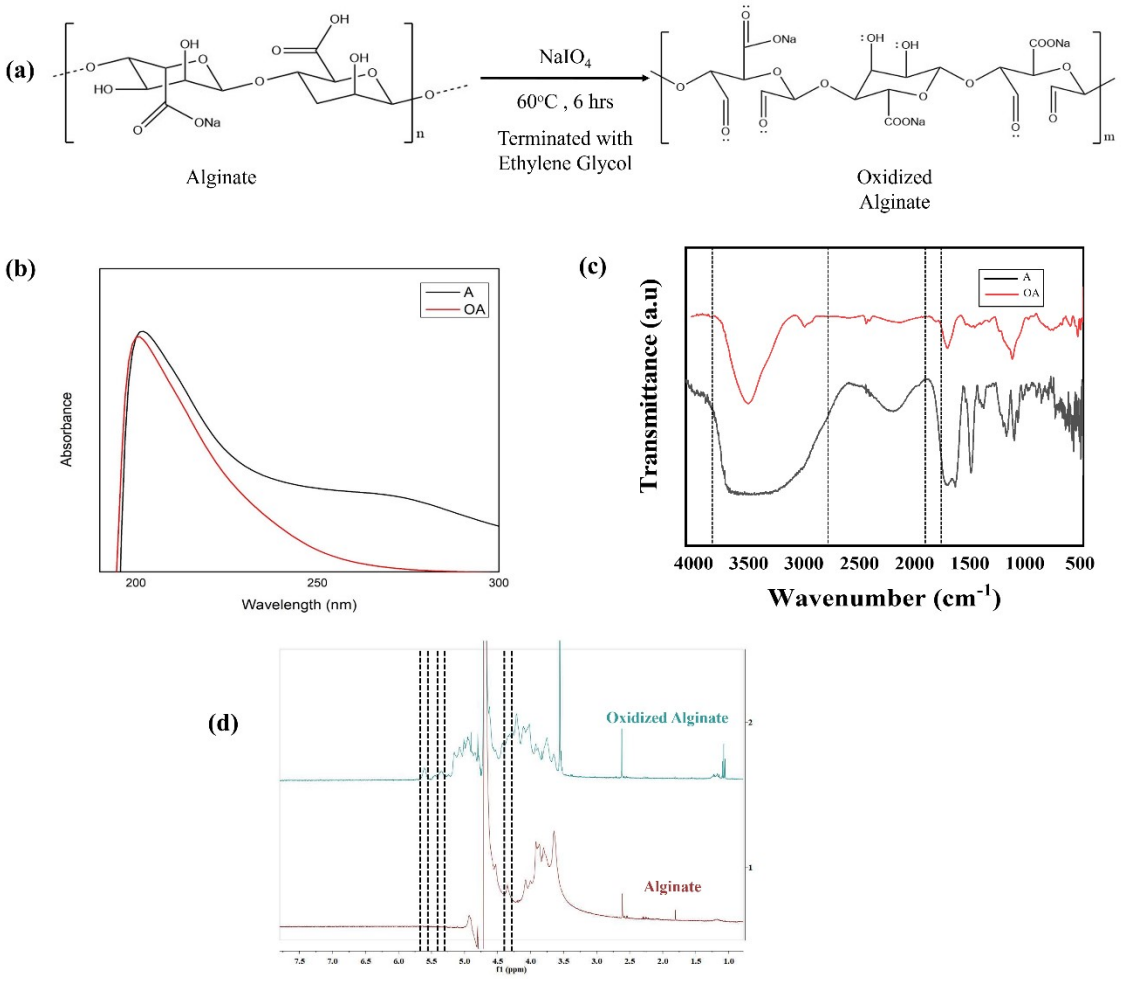

Figure S2. (a) Schematic representation of the oxidation reaction of alginate, showing cleavage of carbon bonds and formation of aldehyde groups, (b) UV-visible spectroscopy analysis demonstrating spectral shifts between alginate and oxidized alginate, (c) FTIR spectra highlighting key functional group modifications after oxidation, (d) ^{1}H NMR spectra showing distinct changes in chemical shifts, confirming the successful oxidation of alginate.

This reaction resulted in the cleavage of the C2 and C3 carbon bonds, replacing them with aldehyde groups in each oxidized group, as previously documented in the literature (Reaction in Figure S1a). Absorption peaks were observed at 205 nm and 270 nm in alginate's UV-visible spectra (Figure S1b). Conversely, in the case of oxidized alginate, a blue shift was noted at 200 nm. Furthermore, the peak at 270 nm disappeared in the oxidized alginate spectrum.

Figure S1c displays the FTIR spectra of alginate and oxidized alginate. Alginate exhibited characteristic peaks at 3428 cm^{-1} (O – H stretching), 2920 cm^{-1} (C – H stretching), 1630 cm^{-1} (C = O stretching), and 1412 cm^{-1} (COO – stretching). However, in the oxidized alginate spectrum, we observed a new peak at 1741 cm^{-1}, corresponding to the symmetric vibration of the aldehyde groups. The band between 3200 and 3600 cm^{-1} narrowed, suggesting modifications in the hydroxyl groups [3].

OA synthesis was confirmed using ^{1}H NMR analysis, as depicted in Figure S1d. The NMR spectrum of alginate displayed peaks ranging from 3.4 ppm to 5.0 ppm. The ^{1}H NMR spectrum shows that the peak at 4.4 ppm observed in alginate disappeared upon oxidation. Furthermore, two new signals emerged at 5.3 and 5.6 ppm, corresponding to hemiacetalic protons formed from aldehydes and their adjacent hydroxyl groups. These observed changes collectively confirmed the formation of OA [4].

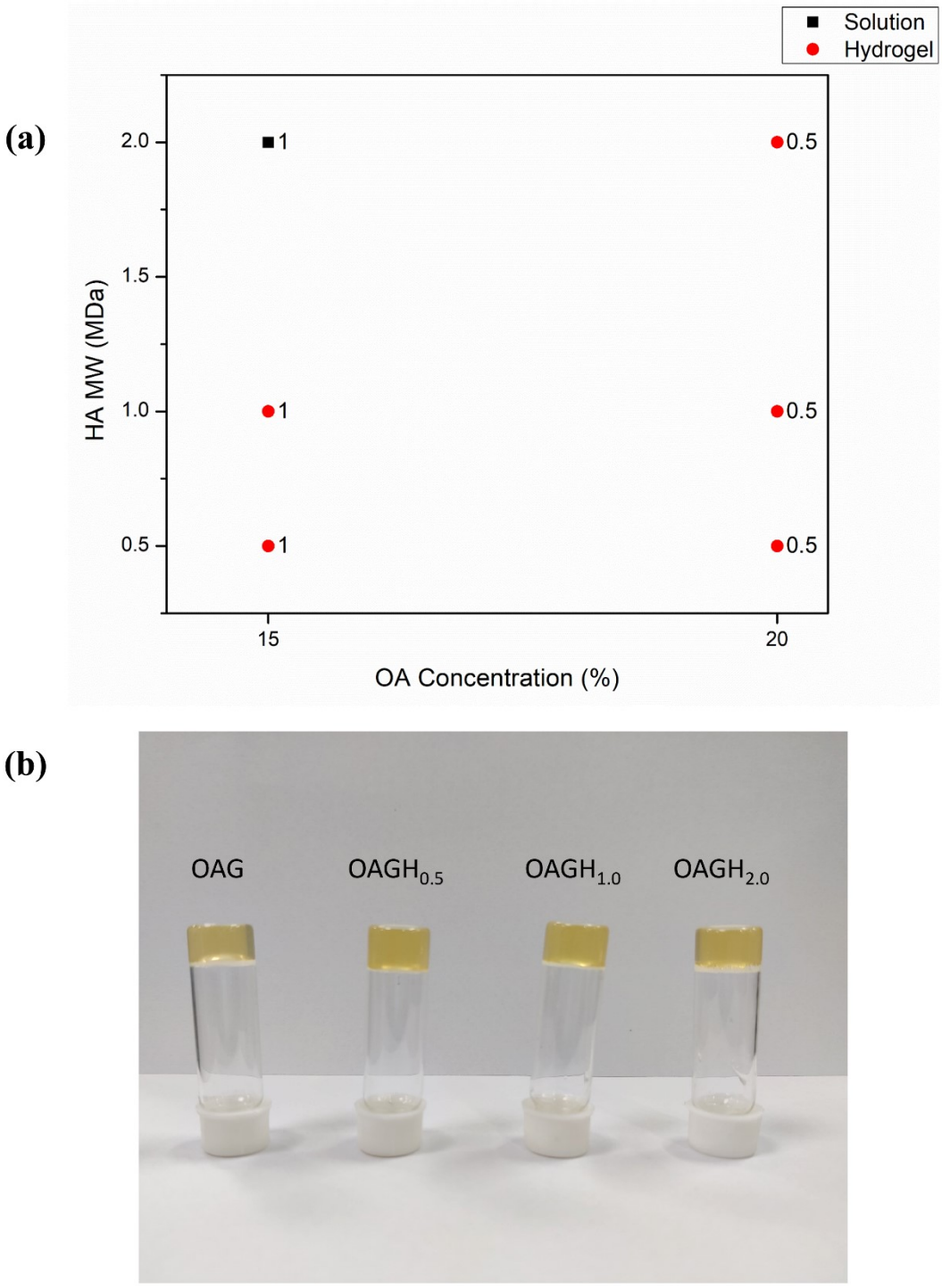

Figure S3 (a) Sol-gel formation of OAGH hydrogels (b)Vial inversion test to check hydrogel formation

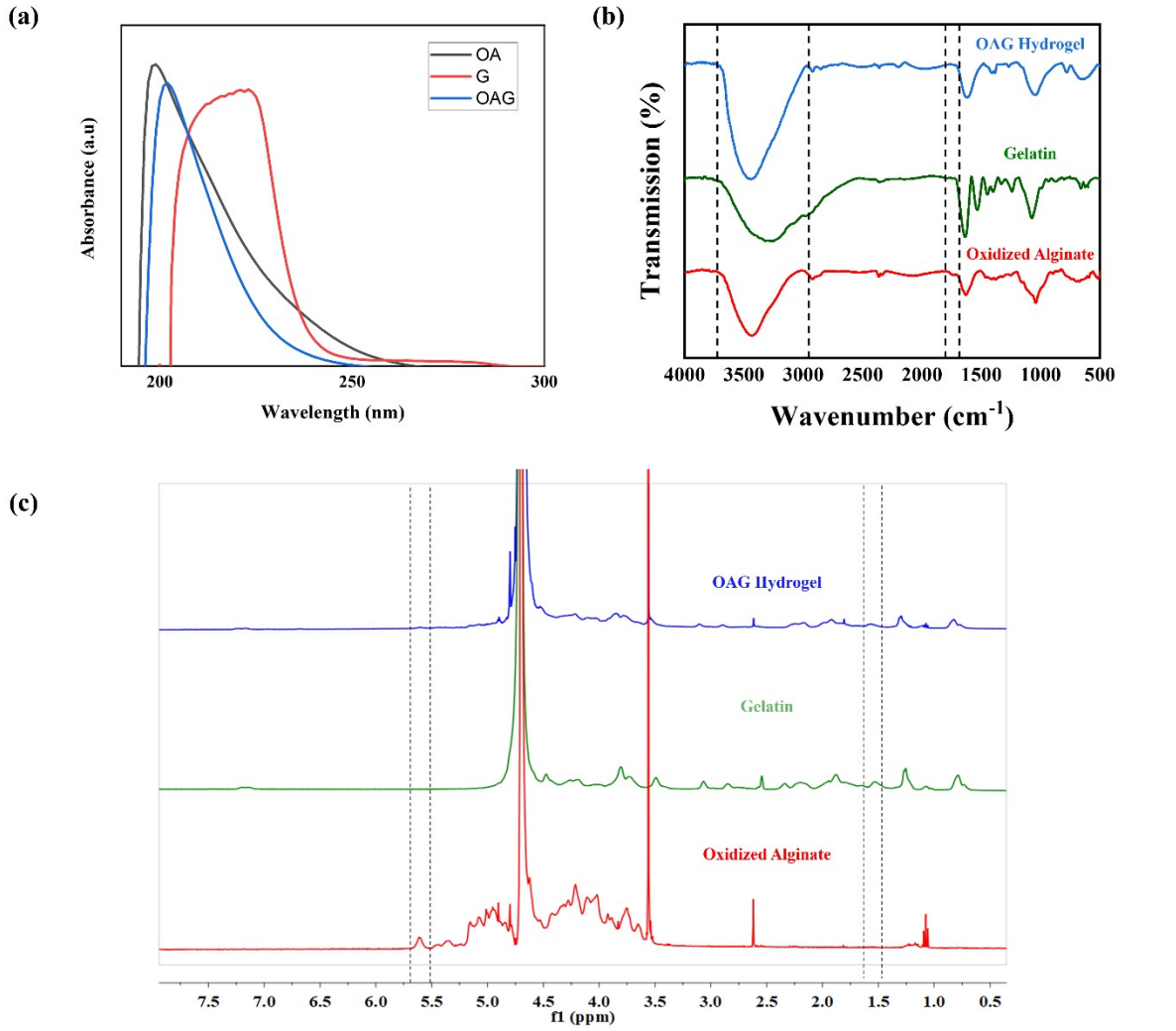

Figure S4 Characterization of OA, G, and OAG hydrogels. (a) UV-visible spectroscopy analysis demonstrating spectral shifts, (b) FTIR spectra highlighting imine bond formation in OAG hydrogel, (c) ^{1}H NMR spectra showing distinct changes in chemical shifts, confirming the formation of imine bonds

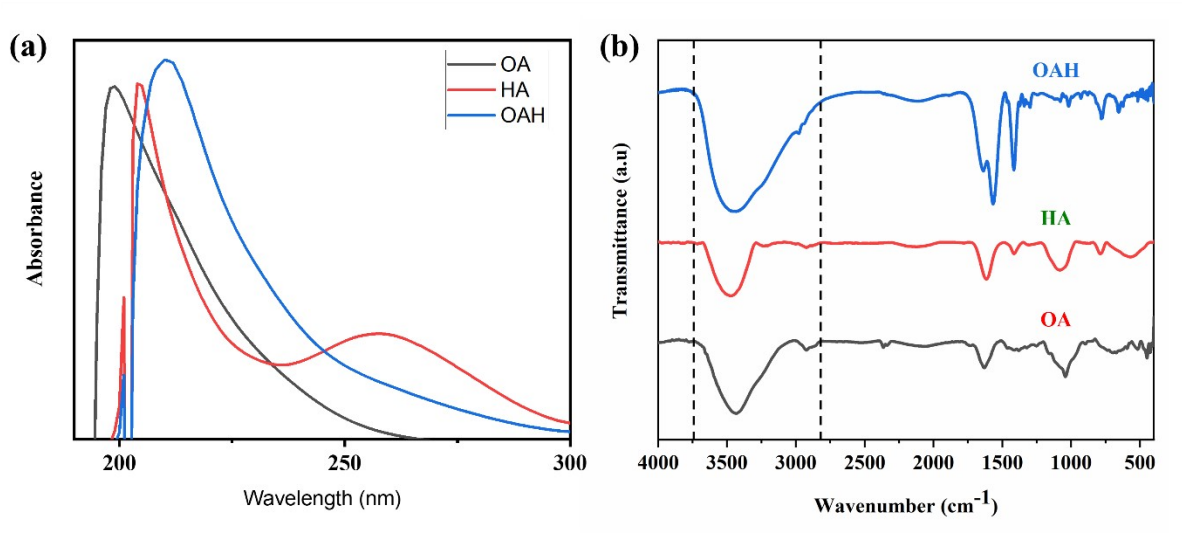

Figure S5 (a) UV-visible spectroscopy of OA, HA, and OAH. The peak disappearance at 260 nm in HA spectra and peak shift from 210 nm to 212 nm in OAH spectra indicates possible interaction between OA and HA, (b) FTIR spectra of OA, HA, and OAH. The spectra show slight shifts in peaks between 3000-3700 cm^{-1} due to the hydrogen bond interaction between OA and HA.

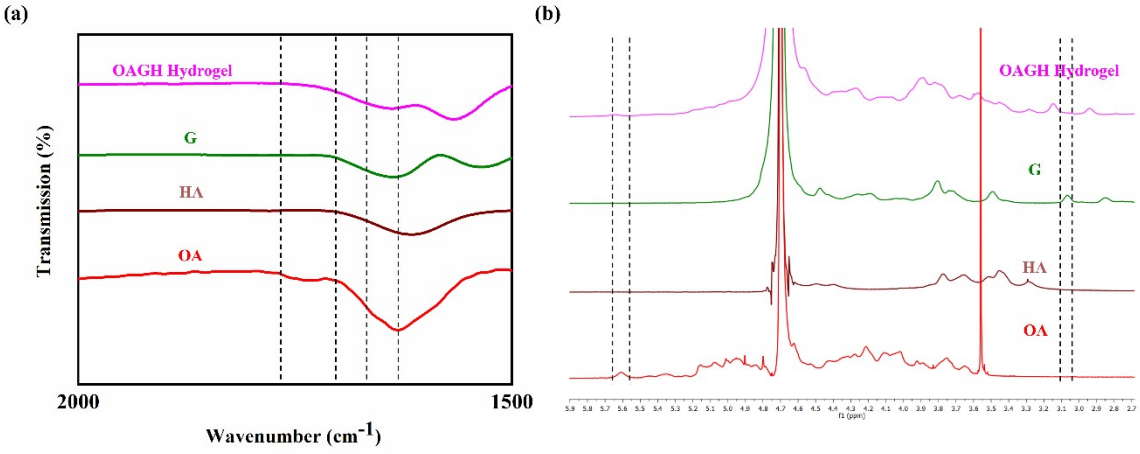

Figure S6 (a) Zoomed-in FTIR spectra highlighting the region between 1500–1800 cm^{-1} for OAG and OAGH hydrogels. The disappearance of peaks at 1740 cm^{-1} (C=O stretching of aldehyde in OA) and 1538 cm^{-1} (N–H bending of amide in gelatin) in OAGH, along with the emergence and shift of a peak at ~1645 cm^{-1}, indicate the formation of imine (Schiff base)

bonds between OA and gelatin and (b) Zoomed-in ^{1}H NMR spectra of OAG and OAGH hydrogels highlighting the chemical shift regions between 2.5–6.0 ppm. The disappearance of the peak at ~5.6 ppm (aldehyde protons of oxidized alginate) and the peak at ~2.8 ppm (primary amine protons of gelatin) in OAGH confirms the formation of imine (Schiff base) bonds between OA and gelatin.

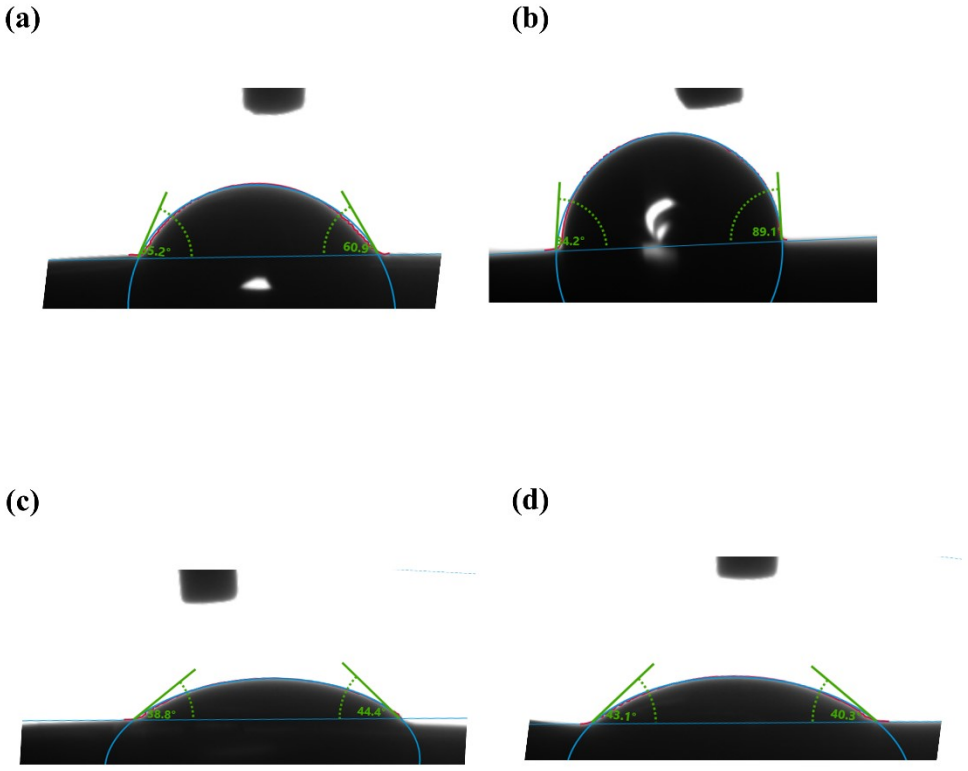

Figure S7 Water contact angle measurements of HA-based hydrogels with different molecular weights. The images show the contact angle of water droplets on the surface of (a) OAG, (b) $OAGH_{0.5}$, (c) $OAGH_{1.0}$, and (d) $OAGH_{2.0}$ hydrogels, illustrating the differences in wettability. The lower contact angle observed for $OAGH_{1.0}$ and $OAGH_{2.0}$ indicates higher hydrophilicity

compared to $OAGH_{0.5}$, which displayed a higher contact angle due to increased crosslinking and reduced water absorption.

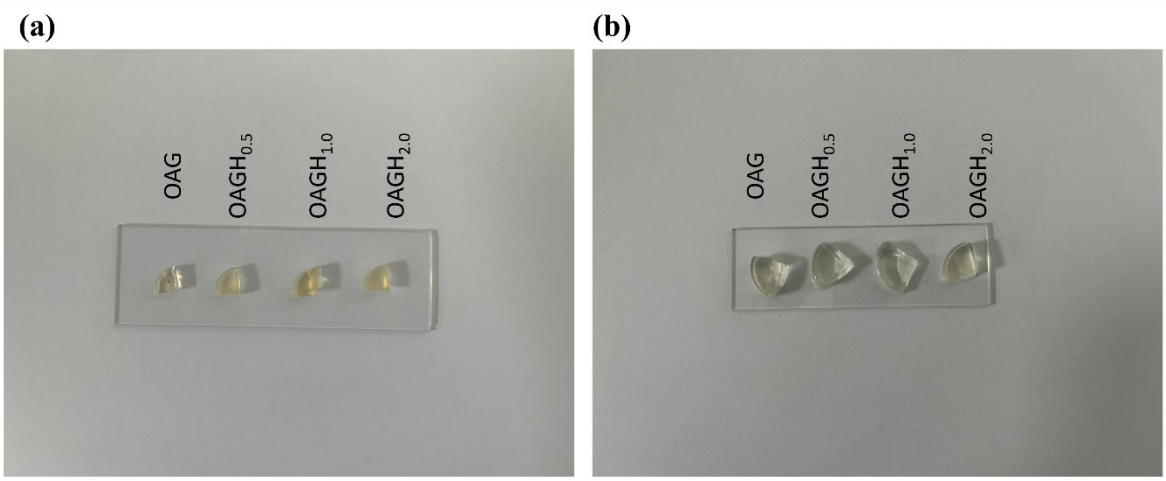

Figure S8 Swelling behavior of the hydrogel in PBS. The image shows the hydrogel (a) before and (b) after swelling in phosphate-buffered saline (PBS), highlighting the increase in volume upon absorption of the PBS solution.

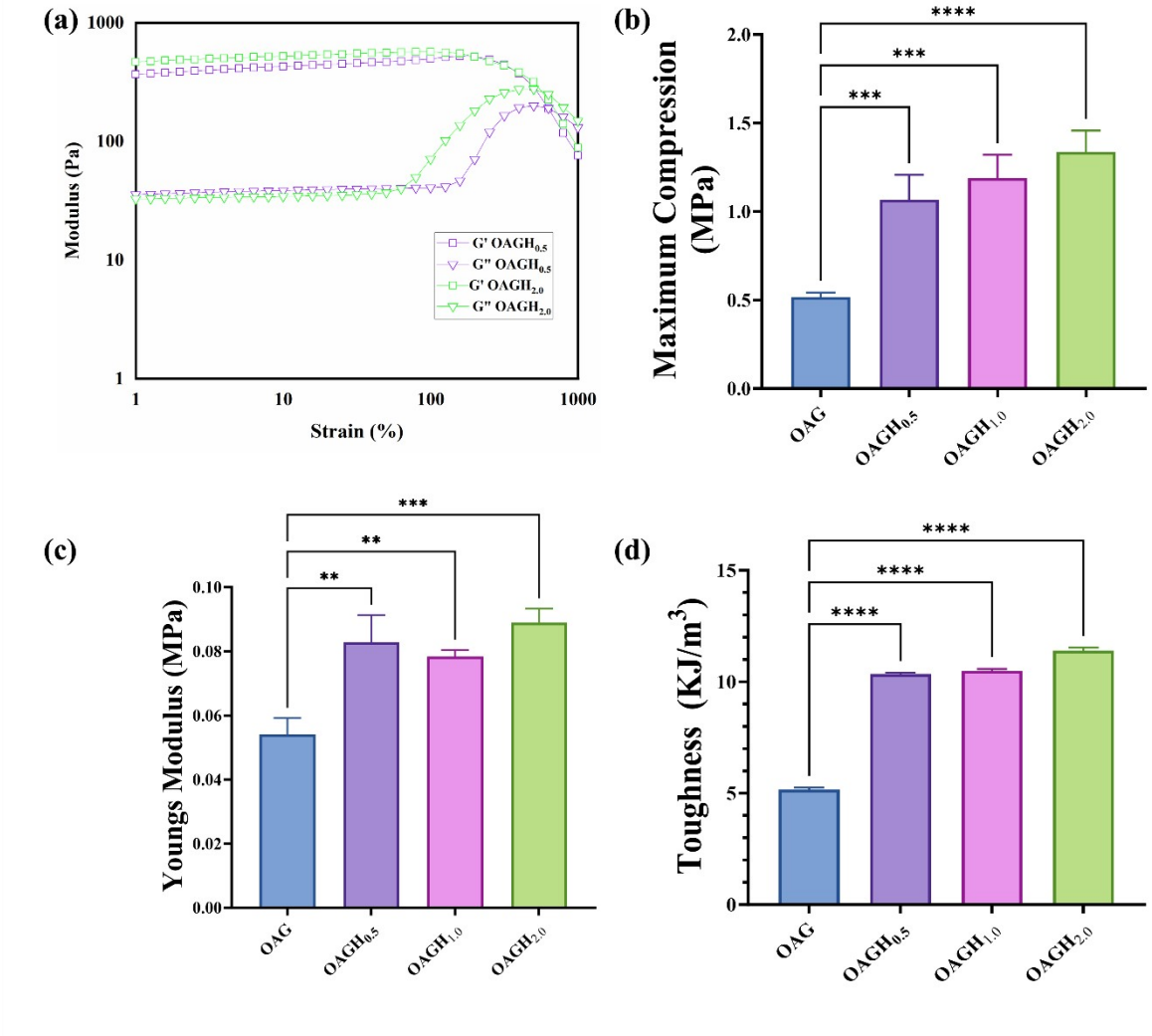

Figure S9 (a) Storage and loss modulus in strain sweeps of $OAGH_{0.5}$ and $OAGH_{2.0}$ hydrogels, (b) Maximum compression strength of the hydrogels, (c) Young's Modulus of the hydrogels, (d) Toughness of the hydrogels

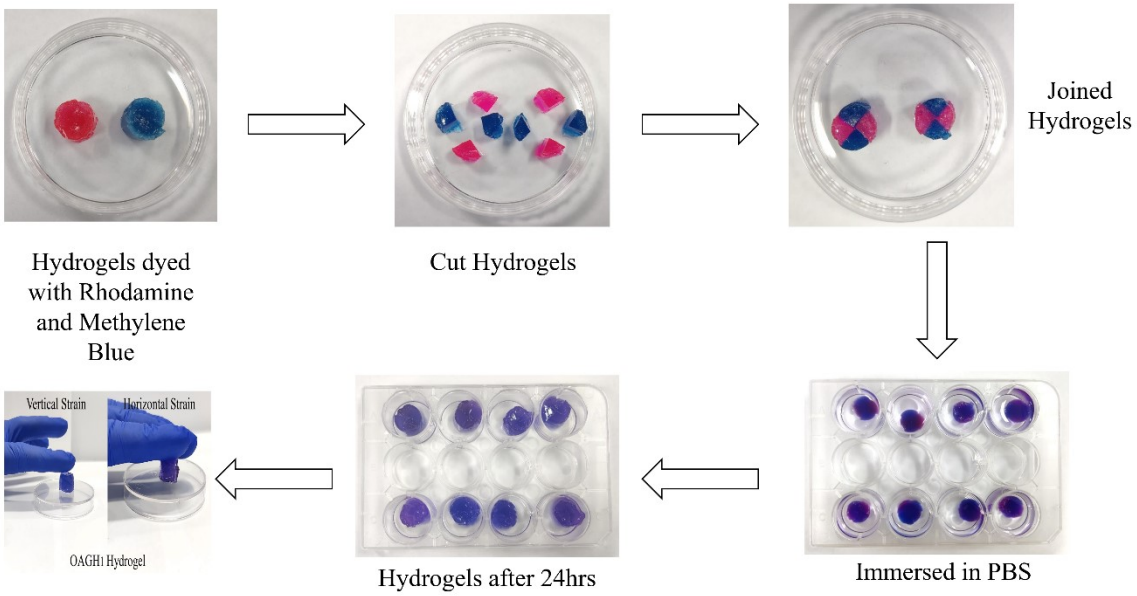

Figure S10 Macroscopic assessment of the self-healing behavior of hydrogels.

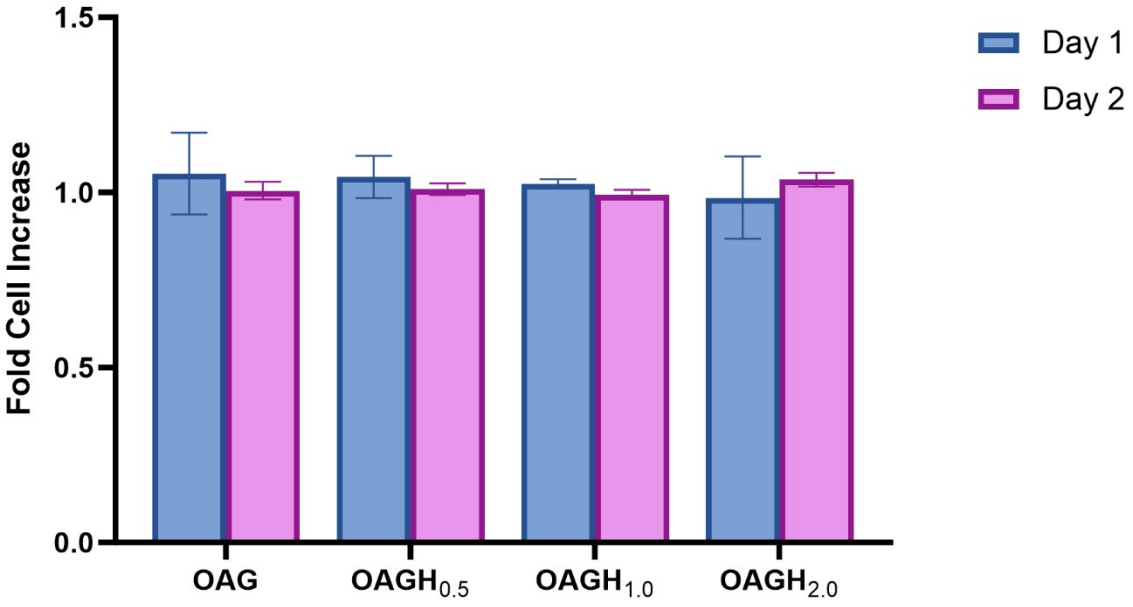

Figure S11 Cytotoxicity evaluation of the hydrogels against L929 cells. The results show no significant reduction in cell viability, indicating that the hydrogels are non-toxic to L929 cells.

Isolation of primary chondrocytes from goat knee cartilage:

Goat knee joints were obtained from a local slaughterhouse. Chondrocytes were extracted from the articular cartilage through enzymatic digestion for approximately 20 h using DMEM/F12 media containing collagenase type II and 1% penicillin/streptomycin. Digestion was halted with FBS-containing media, and the suspension was filtered using a 70 µm cell strainer. The isolated cells were cultured in DMEM/F12 media supplemented with 10% FBS and 1% antibiotic/antimycotic solution.

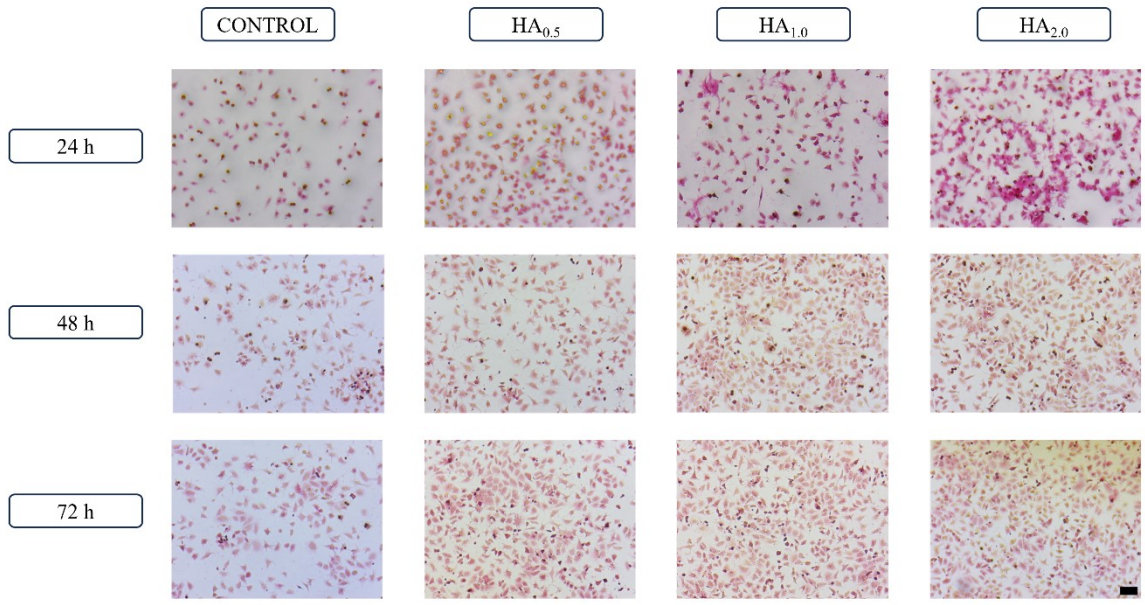

Figure S12 The figure shows Sirius red staining of chondrocytes cultured in the presence of HA with various molecular weights. Chondrocytes exposed to HA exhibited similar levels of collagen expression and an increased number of cells capable of producing collagen, as indicated by the Sirius red staining. Magnification: 10× and Scale bar: 200 µm

References:

1 P. Jeeva, S. Shanmuga Doss, V. Sundaram and G. Jayaraman, *Appl Microbiol Biotechnol*, 2019, **103**, 4363–4375.

2 K. Puvendran and G. Jayaraman, *Appl Microbiol Biotechnol*, 2019, **103**, 6989–7001.

3 C. K. Balavigneswaran and V. Muthuvijayan, *ACS Appl Bio Mater*, 2021, **4**, 5362–5377.

4 L. Wang, Y. Hou, X. Zhong, J. Hu, F. Shi and H. Mi, *Carbohydr Polym*, 2018, **208**, 42–49.